

Quantifying Frictional Losses for a 2-Degree-of-Freedom Energy-Efficient Walking Robot

Konrad Ahlin, Mario W. Gomes

Rochester Institute of Technology
76 Lomb Memorial Drive, Rochester NY, 14623 USA
kja1497@rit.edu; mwgeme@rit.edu

Abstract - A modern goal of walking robots is to achieve motion while maintaining relatively low energy costs. Traditional robots are capable of level ground walking, but they are generally not energy efficient. The Extended Body Rimless (EBR) wheel is a robotic walking device which employs torsional springs and a rotating pendulum to prevent energy from being lost due to foot collisions. In simulations without friction, the EBR wheel has a periodic motion, across level ground, which can completely eliminate energy loss. However, when non-conservative forces are introduced in the system, the periodic motion of the EBR wheel is broken and an external energy source is required. To minimize the cost of transport of the system, the source and magnitude of the friction loss must be understood. Experimental trials coupled with models for the sources of drag have indicated that air drag from the rotating pendulum is a primary source of friction, accounting for about 30% of the energy loss when moving. Air drag is not often considered in robotic walkers, but for fast moving devices, drastic improvements in energy efficiency can be obtained if aerodynamic issues are addressed.

Keywords: Walking, energy efficiency, collisions, air-drag, passive dynamic walking, rimless wheel.

1. Introduction

Bipedal walking is a complex coordinated motion. Designing a machine to walk without falling down is a difficult task, but designing a machine to walk *with a human-like gait* is an even more difficult task. Until recently, the goal of human-like walking has been the aspiration of many who work in the robotics community. However, the amount of energy used by a walking robot outside of simulations has not received as much of a focused effort.

Many designers have worked to create mechanically simple, passive and active walking robots. McGeer (1990) has shown with his kneed-biped walker that passive robots can have periodic, stable walking gaits without direct position control over their limbs. McGeer's models rely on careful mechanical design and specific initial conditions and their resulting gaits are remarkably human-like, stable, and require little input power. Mechanically simpler models also have stable walking gaits. Asano (2012) details the dynamics and inherent stability of a simple rimless wheel. Expanding on the concept of the simple rimless wheel, Asano has also designed a rimless wheel with telescoping legs and a control system that are capable of level ground motion (Asano2009). While Asano's telescoping wheel augments the simple rimless wheel concept with telescoping legs and a control scheme, others, such as Ozawa and Kojima (Ozawa 2010) rely entirely on control methods to let a compass walker traverse various slopes, including level ground. All of these designs use mechanics or controls to maintain periodic motion with a low cost of transport.

The dynamics of a rimless wheel has been studied extensively by other researchers. For example, Jiao *et al.* (2011) examined a variant of the rimless wheel which had asymmetric flat feet, resulting in two impacts per leg (heelstrike and toestrike). In addition, Byl and Tedrake (2009) studied the dynamics of a rimless wheel moving down a ramp with randomly generated roughness. Although the rich dynamics of even this simple system are of interest by themselves, an improved understanding of how this simple system moves has led to advances in understanding the dynamics of bipedal walking robots.

When any creature or machine walks, the impact of a foot hitting the ground will dissipate energy. However, Chatterjee *et al.* (2007) have shown that an object could be designed whose inherent dynamics allow for uncontrolled motions which avoid energy dissipative collisions in one dimension. Chatterjee *et al.* demonstrated that a collision that occurs at zero velocity will not dissipate energy. Gomes and Ruina (2011) have expanded this concept of collisionless impacts to simulated "walking" models to show that collisionless motion can be applied to bipedal robots moving in multiple dimensions. The Extended Bodied Rimless (EBR) wheel also takes advantage of collisionless motion to walk in multiple dimensions but with a relatively simple design (Gomes 2005). In simulation, the path of the EBR wheel is periodic, allowing for the system to continue walking indefinitely on level ground without energy input. The relatively simple design of the EBR wheel makes it a prime candidate for testing the concept of collisionless motion in experimentation to create a low cost of transport walking robot.

Although the periodic path of the EBR wheel may exist in simulation, the periodic nature of the system is lost once friction is considered. Most models of walking robots do not consider energy lost due to forces such as air-friction and non-elastic deformations of the limbs, but even these often neglected losses in energy mean that a physical EBR wheel cannot travel indefinitely on level ground without energy input.

To reduce energy losses in the model, the dominant forms of friction in the system must first be understood. The EBR wheel has three essential parts: the outer frame, the inner oscillating pendulum, and the torsional springs. Any energy lost from the system must be coming from one of these three systems. To simplify the investigation, the outer frame will be excluded from consideration of energy losses. Once the primary forms of friction in the system are understood, the necessary changes can be made to the overall design to improve performance.

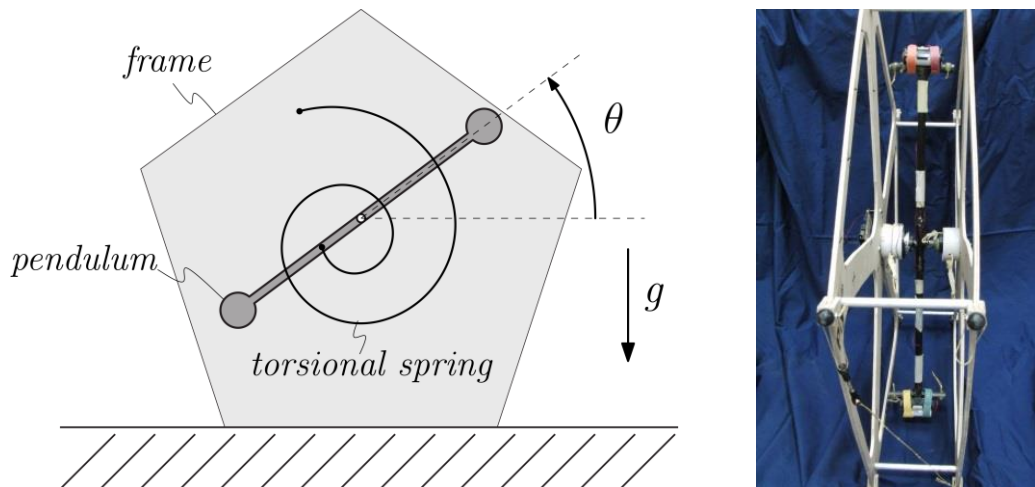


Fig. 1. LEFT: Extended Bodied Rimless wheel diagram, the frame and pendulum are coupled by a torsional spring system. RIGHT: Pendulum system in current prototype, note: springs have been removed for clarity.

2. Pendulum Energy Loss, “Coasting Trials”

To determine how much energy is being lost from the pendulum alone, 20 trials were performed without the torsional spring system, allowing the pendulum to freely coast on its axis; these trials will be referred to as “coasting trials”. An encoder disk with 0.18° resolution was attached at the central hub to measure the rotational position of the pendulum during these experiments. The centre of mass of the pendulum is less than 5 mm from the axle.

2. 1. Air Drag Model

The air drag model used for the first part of the analysis is represented in Eq. 1, where I_{com} is the mass moment of inertia about the center of mass, c_a is the air drag coefficient, and θ is the absolute angular position of the pendulum.

$$I_{com} \frac{d^2\theta}{dt^2} + c_a \left(\frac{d\theta}{dt}\right)^2 = 0 \quad (1)$$

Solving for this separable ordinary differential equation (ODE) and using the initial conditions of $\theta(t=0) = 0$ and $\frac{d\theta}{dt}(t=0) = \dot{\theta}_0$ yields the solution shown in Eq. 2.

$$\theta(t) = \frac{I_{com}}{c_a} \ln\left(\frac{c_a}{I_{com}}t + \frac{1}{\dot{\theta}_0}\right) - \ln\left(\frac{1}{\dot{\theta}_0}\right) \quad (2)$$

Fig. 2 demonstrates how the analytical equation for air drag compares against the experimental results, assuming a best-fit relationship to determine the air drag coefficient c_a . The initial velocity is numerically calculated from the position data.

From these sets of trials, the average air drag coefficient experienced by the pendulum is $c_a = 1.42 \cdot 10^{-4} \text{ kg}^1 \text{ m}^1 \text{ rad}^{-2}$. As can be seen by Fig. 2, the air drag model shown in Eq. 1, fits the experimental data well. The least squares values comparing the experimental data and the analytical estimation are larger than 0.99 for all 20 trials. The success of the analytic model to describe the angular position suggests that air drag is the primary source of friction experienced by the pendulum when freely coasting.

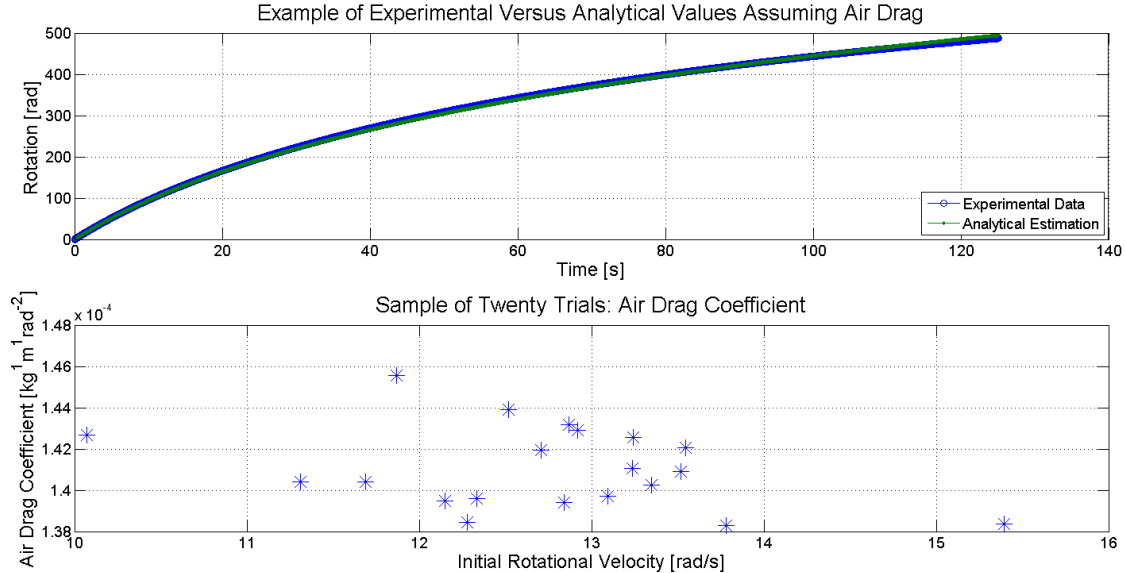


Fig. 2. TOP: Comparison of Experimental trial and air drag analytical representation. BOTTOM: Curve-fit estimations for air-drag coefficients

2. 2. Viscous Damping Model

In addition to the air drag model, the path of motion was estimated assuming viscous damping. The pendulum uses standard ball-bearings to reduce friction on its rotation axis. However, bearings are not

ideal and they may be a source of energy loss in the system. The general model for viscous drag acting on an inertia is shown in Eq. 3, where c_v is the viscous damping coefficient.

$$I_{com} \frac{d^2\theta}{dt^2} + c_v \frac{d\theta}{dt} = 0 \quad (3)$$

Solving the ordinary differential equation, Eq. 5, with the initial conditions of $\theta(t = 0) = 0$ and $\frac{d\theta}{dt}(t = 0) = \dot{\theta}_0$ yields Eq. 6.

$$\theta(t) = \frac{I_{com}}{c_v} \dot{\theta}_0 \left(1 - e^{-\frac{c_v}{I_{com}}t}\right) \quad (4)$$

Fig. 3 demonstrates that the motion of a viscously damped system is similar to the observed path of the pendulum. The analytical solution shown in Eq. 4 is relatively accurate, with an average least squares value of better than 0.9 compared to the experimental data. However, the air drag model fits the experimental data better than the viscous drag model.

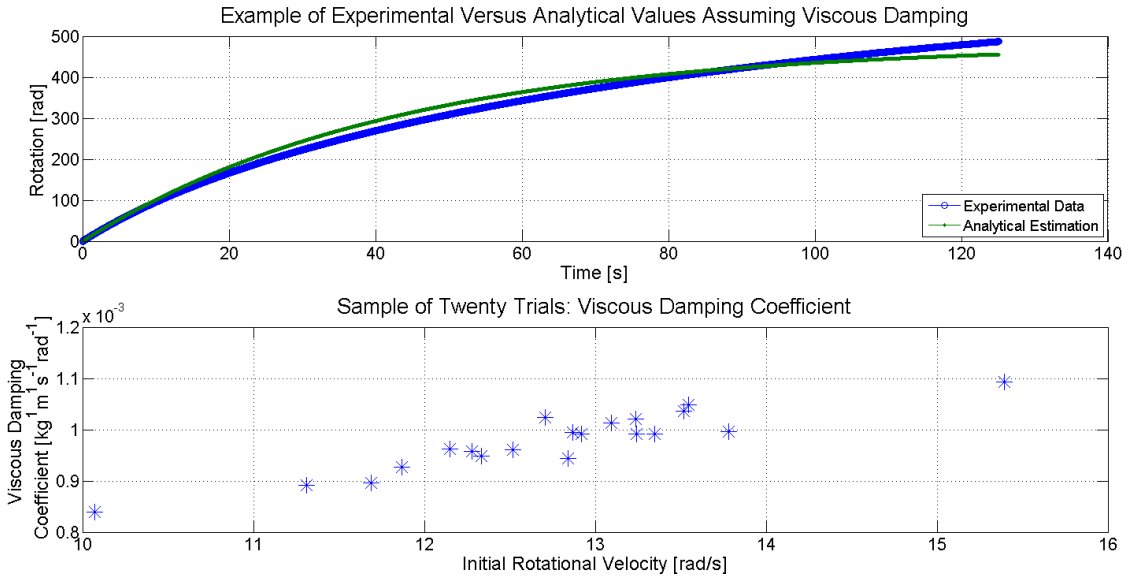


Fig. 3. TOP: Comparison of Experimental trial and viscous damping analytical representation. BOTTOM: Curve-fit estimations for viscous damping coefficients

2. 3. Energy Lost from the Pendulum due to Air Drag

Air drag is the primary source of friction on the freely rotating pendulum. However, it is also interesting to note that the energy loss from the system can be correlated to the instantaneous rotational velocity of the pendulum. Using this correlation we can predict the energy loss due to air drag from the pendulum at higher speeds. Eq. 5 shows how energy loss can be calculated and Eq. 6 shows the estimated energy equation for small differences in rotational position, θ . In these equations, τ_a is the torque due to air drag and E is the energy lost from the pendulum.

$$E = \int_{\theta_1}^{\theta_2} \tau_a \cdot d\theta \quad (5)$$

$$E \approx \frac{1}{2} (\theta_2 - \theta_1) * (\tau_{a2} + \tau_{a1}) \quad (6)$$

From Eq. 6, the energy lost per degree of travel is calculated and compared against the instantaneous rotational velocity of the pendulum, shown in fig. 4. Furthermore, a correlation between energy losses from air drag and pendulum velocity can be observed. A linear approximation to the data is represented in Eq. 7, which was used to extrapolate energy loss from the system due to pendulum air drag at higher speeds; $\dot{\theta}$ is the rotational velocity of the pendulum.

$$\frac{E}{Deg} \approx (2.478 * 10^{-6}) * \dot{\theta}^2 \quad (7)$$

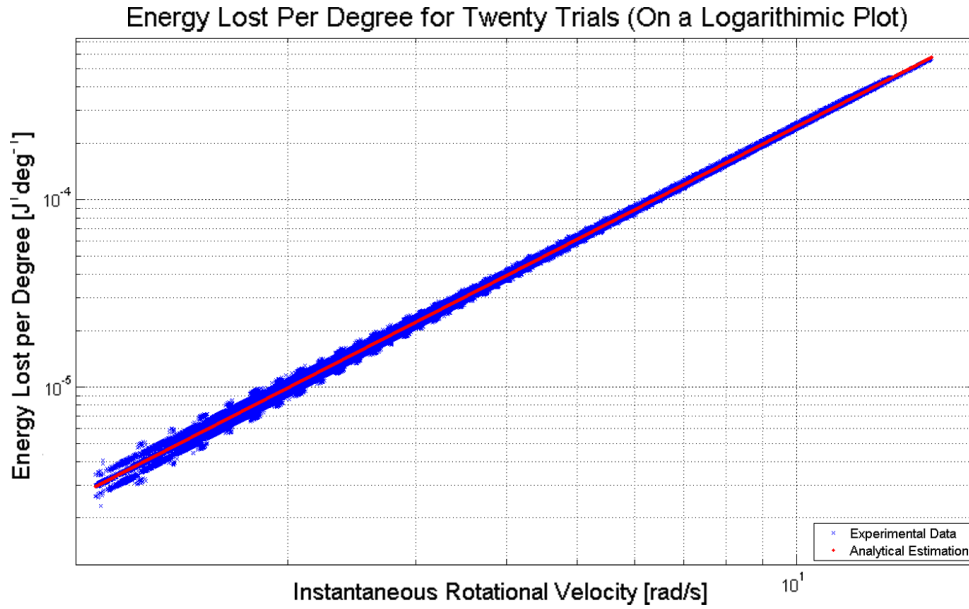


Fig. 4. Energy lost per degree as a function of rotational speed

3. System Energy Loss, “Oscillating Trials”

The pendulum is not the only system in the EBR wheel which might dissipate energy. The torsional spring system could also contribute to the energy losses of the system. The spring system creates a larger cross section for air drag, and the set-up uses strings and springs which may be dissipating energy through slipping. Several sets of oscillating trials were performed with the torsional springs and pendulum while an encoder recorded the rotational position. The rotational velocity was then numerically determined from the position data by a polynomial curve fit to a moving window of data. This curve fit was then analytically differentiated and then used to determine the approximate angular velocity for the central data point in the data window.

3. 1. Air Drag Model

The equations of motion for an oscillating pendulum experiencing air drag are represented in Eq. 8, with k as the torsional stiffness of the springs.

$$I_{com} \frac{d^2\theta}{dt^2} + c_a \left(\frac{d\theta}{dt}\right)^2 + k\theta = 0 \quad (8)$$

This non-linear ODE does not have a standard solution, but the path of motion can be estimated using numeric simulations.

Fig. 5 shows a comparison of the experimental data versus simulated results. The "Analytically Estimated" air drag model uses the drag coefficients from the coasting trials: $1.42 \cdot 10^{-4} \text{ kg}^1\text{m}^1\text{rad}^{-2}$, and the "Analytically Approximated" model uses an air drag value based on the experimental results, $7.5 \cdot 10^{-3} \text{ kg}^1\text{m}^1\text{rad}^{-2}$.

Fig. 5 shows that there must exist within the system more non-conservative forces than simply the air drag from the pendulum. Assuming a higher drag coefficient fits the model better, but Fig. 5 shows that even a model with a relatively high air drag coefficient will soon diverge from the experimental results. Thus, if air drag is not an appropriate representation for the system, another model must be applied.

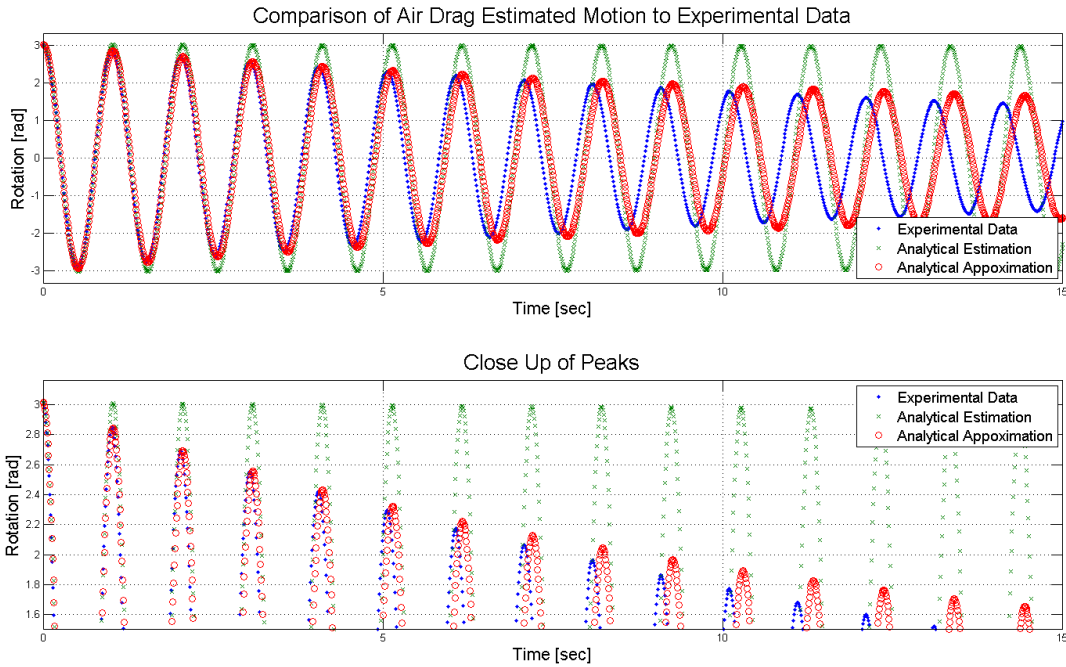


Fig. 5. TOP: Comparison of experimental data, air drag simulation using the analytically estimated air drag from coasting trials: $1.42 \cdot 10^{-4} \text{ kg}^1\text{m}^1\text{rad}^{-2}$ and an analytically approximated air drag to better represent the model: $7.5 \cdot 10^{-3} \text{ kg}^1\text{m}^1\text{rad}^{-2}$. BOTTOM: Close up of peaks to show accuracy of model.

3. 2. Viscous Damping Model

The coasting experiments indicated that air drag dominates the energy loss in the system. The viscous damping model is not meant to represent directly the types of friction within the system. Rather, the viscous model is an attempt to accurately predict the motion of the torsional springs and pendulum considering all of the inherent friction observed from experimentation. Eq. 9 shows the form of the model we used for the oscillating system assuming viscous damping.

$$I_{com} \frac{d^2\theta}{dt^2} + c_v \frac{d\theta}{dt} + k\theta = 0 \quad (9)$$

Using a viscous damping model has one great advantage over the equations of motion for air drag: the viscous damping differential equation can be solved analytically, which allows for a simple curve fitting routine to estimate the damping coefficient. An example of experimental data compared with an estimated path of motion using viscous damping is shown in Fig. 6.

Although the source of friction is not completely defined, it is clear from Fig. 6 that a viscous damping model accurately predicts the motion of the torsional pendulum. However, without directly

understanding all the sources of friction, it is still unclear as to how best reduce the energy losses of the system.

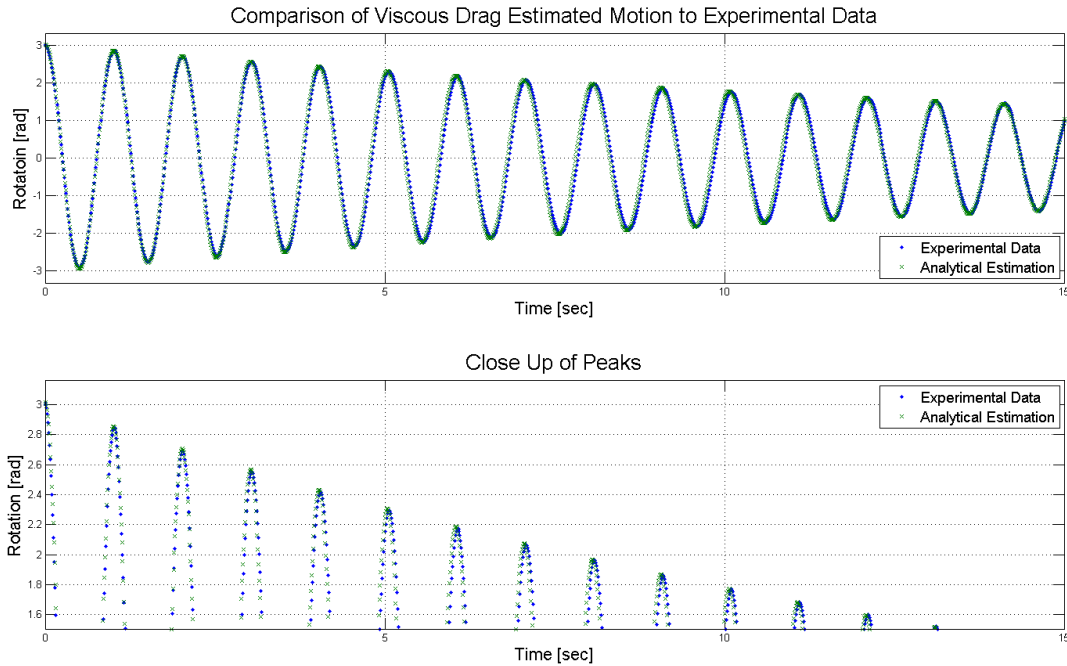


Fig. 6. TOP: Comparison of experimental data and viscous drag model using an analytically calculated damping coefficient. Bottom: Close up of peaks to show accuracy of model.

3. 3. Pendulum Energy Loss Comparison

Even though a viscous damping model might accurately predict the position of the torsional pendulum, it is still prudent to know how much energy is lost purely from the air drag caused by the rotating pendulum during an oscillation. The current pendulum was not designed to be aerodynamic. Eq. 7 was used to estimate how much energy was lost per oscillation of the torsional pendulum due to air drag per degree. A comparison between the actual kinetic energy losses per oscillation from the experiments and the estimated energy loss due to air drag is shown in Fig. 7.

Fig. 7 clearly shows the role of air drag in the oscillating pendulum. As the angular velocity of the pendulum increases, the portion of energy loss from air drag decreases. The current EBR wheel prototype has a peak rotational velocity per oscillation of about 27 rad/sec. At this speed, and using this model for air drag, we predict that the system will lose nearly 30% of its energy loss from the pendulum air drag alone.

4. Conclusion and Further Work

For the coasting trials with the pendulum, air drag is a significant source of frictional losses. The air drag coefficient for the pendulum alone is about $1.42 \cdot 10^{-4} \text{ kg}^1\text{m}^1\text{rad}^{-2}$. Although this air drag value accurately represents the coasting trials, the system appears to undergo a drastic change with the torsional springs attached. For the oscillating trials, air drag no longer accurately predicts the motion of the pendulum. Instead, a viscous damping model matched the experimental oscillation trials with a high degree of accuracy. The angular position of the pendulum in the experiments can be accurately predicted, but the viscous damping model does not give insight into all of the sources of friction in the system. However, comparing expected losses from pendulum air drag reveals that about 30% of the total energy loss of the system is coming directly from the pendulum moving through the air. Redesigning the pendulum to be more aerodynamic should allow for a significant increase in system performance.

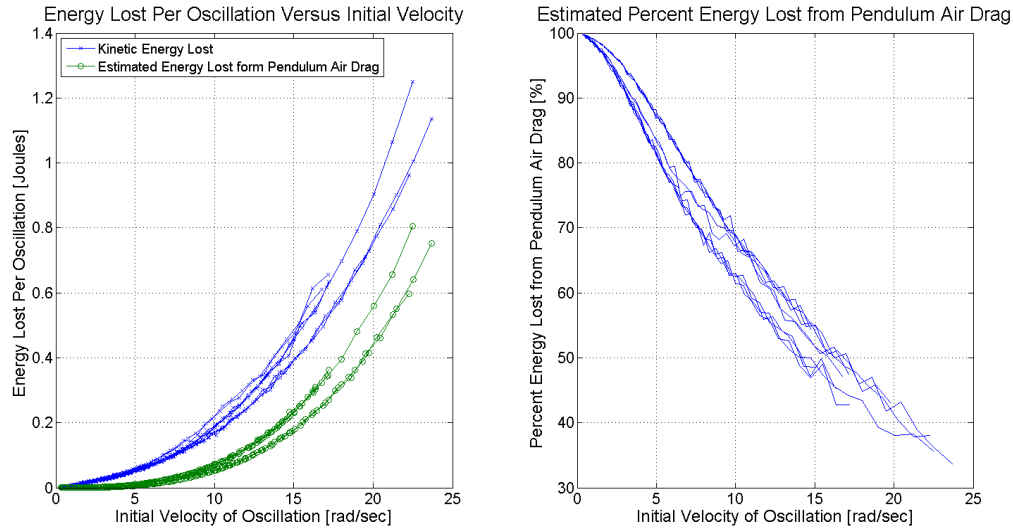


Fig. 7. LEFT: Comparison of energy lost per oscillation versus initial velocity of oscillation against expected energy lost from pendulum air drag. RIGHT: Percentage of energy lost per oscillation attributed to pendulum air drag.

Walking robot models do not usually include the effects of air drag on the system, but because the EBR wheel is moving quickly and attempting to reach minimize energy loss, air drag plays an important role in the model, and its effects must be considered.

References

- Asano, F. (2009). Dynamic Gait Generation of Telescopic-legged Rimless Wheel Based on Aymmetric Impact Posture. "2009 9th IEEE -RAS International Conference on Humanoid Robots", 68-73.
- Asano, F. (2012). Stability principle underlying passive dynamic walking of rimless wheel. "2012 IEEE International Conference on Control Applications", 1039-1044.
- Byl, K., & Tedrake, R. (2009). Metastable Walking Machines. "The International Journal of Robotics Research", 28(8), 1040–1064.
- Chatterjee, A., Pratap, R., Reddy, C., and Ruina, A. (2007). Persistent Passive Hopping and Juggling is Possible Even With Plastic Collisions. "The International Journal of Robotics Research" 21, 7, 621-634.
- Jiao, J., Zhao, M., & Mu, C. (2010). Rimless Wheel with Asymmetric Flat Feet. "Proceedings of the 2010 IEEE International Conference on Robotics and Biomimetics", Dec 14-18, pp. 288–293.
- Kuo, A. (2007). Choosing your steps carefully. "IEEE Robotics & Automation Magazine" 14, 2, 18-29.
- Gomes, M. (2005). Collisionless rigid body locomotion models and physically based homotopy methods for finding periodic motions in high degree of freedom models. PhD thesis, Cornell University.
- Gomes, M., and Ruina, A. (2011). Walking Model with no Energy Cost. "Physical Review E" 83, 3 032901.
- McGeer, T. (1990). Passive walking with knees. "Proceedings of the IEEE International Conference on Robotics and Automation", 1640-1645.
- Ozawa, R., and Kojima, Y. (2010). Control of a Powered Planar Biped without Ankle Actuation. "Intelligent Robots and Systems IROS 2010 IEEE/RSJ International Conference", 3617-3622.